A thermodynamic model for feldspars in $KAlSi_3O_8$–$NaAlSi_3O_8$–$CaAl_2Si_2O_8$ for mineral equilibrium calculations

Tim JB Holland[1], Eleanor CR Green[2] & Roger Powell[2]

[1]Department of Earth Sciences, University of Cambridge, Cambridge, CB2 3EQ, UK

[2]School of Geography, Earth and Atmospheric Sciences, The University of Melbourne, Victoria 3010, Australia

Corresponding author: tjbh@cam.ac.uk

Short title: Thermodynamic model for feldspars

Abstract

Activity-composition (*a*-*x*) relations for feldspars for petrological calculations in $KAlSi_3O_8$–$NaAlSi_3O_8$–$CaAl_2Si_2O_8$ are calibrated using literature data for (i) plagioclase cation-exchange experiments at 600 and 700°C, (ii) experimental ternary feldspar pairs at 880-900°C, (iii) the alkali feldspar solvus, and (iv) the dry melting loop for plagioclase. The results are tested against the calorimetric heat of solution data and the experimental pressures for plagioclase coexisting with grossular, wollastonite and quartz. As the aim is to produce *a*-*x* relations suitable for petrological modelling, we do not attempt to model complex structural phenomena in feldspar, except where they appear to contribute significantly to the energetics of high-temperature mixing. Seven models were investigated, using various formulations of entropy of mixing together with the van Laar model for non-ideal mixing. The model (4TR) that most satisfactorily reproduces the experimental data is one in which Al and Si partially order onto the four tetrahedral sites, approximated by reducing the tetrahedral site entropy of mixing by a factor of four. When combined with an ordered albite this model allows a peristerite gap closing at 600°C at the albite composition. The resulting activity-composition relations for feldspar should be applicable in petrological phase equilibrium calculations over a large range of geologically-relevant pressure and temperature.

KEYWORDS feldspars, activity-composition relations, equilibrium thermodynamics

1 Introduction

Feldspars are ubiquitous in crustal and uppermost mantle rocks, so it is of fundamental importance that petrological phase equilibrium modelling should approximate their thermodynamics appropriately. Yet the plagioclase solid solution shows exceptional structural complexity, including phase transitions, extensive short-range order, and "long-range order" (aperiodic, incommensurate ordering), and is still being characterised by mineralogical experiments (e.g. Jin *et al.*, 2019; Jin & Xu, 2017; McConnell, 2008; Carpenter, 1994; Carpenter & McConnell, 1984).

Numerous thermodynamic models have been proposed that reflect at least part of the complexity of structural change across the plagioclase solid solution (e.g. Ghiorso 1984, Green & Usdansky 1986, Fuhrman & Lindsley 1988, Elkins & Grove 1990, Holland & Powell 1992, Holland & Powell 2003, Benisek *et al.* 2010). For example, Holland & Powell (1992) represented the $C\bar{1}$–$I\bar{1}$ transition, using two models that were made contiguous at the transition.

In this paper we revisit the modelling of plagioclase for phase equilibrium calculations. Since our purpose is petrological modelling, we seek a simple model. Our goal is not primarily to represent the complexity of feldspar structures – in this case the simpler models (see below) can describe the mixing properties as well as or better than the more complex ones investigated. We require our model to satisfy the following key experimental constraints: (a) experimental cation-exchange data for plagioclase-($NaCl$-$CaCl_2$) fluid (Orville 1972, Schliestedt & Johannes 1990); (b) alkali feldspar solvus at various pressures (Orville 1963, Luth & Tuttle 1966, Goldsmith & Newton 1974); (c) experimental ternary feldspar pairs (Elkins & Grove 1990); and (d) the plagioclase melting loop at 1 bar (Bowen 1913).

2 Structure of feldspars

In plagioclase feldspar there are four tetrahedral sites on which Al and Si atoms are distributed. The ordering process can be envisaged as occurring in two stages with decreasing temperature. In the first stage the Al and Si are distributed over two t1 and two t2 sites within the structure (Fig. 1). The order parameter for this process, designated Q_{t}, following Carpenter and Salje (1994), can be defined as

$$Q_{\mathrm{t}} = \frac{X_{\mathrm{Al}}^{\mathrm{t1}} - X_{\mathrm{Al}}^{\mathrm{t2}}}{X_{\mathrm{Al}}^{\mathrm{t1}} + X_{\mathrm{Al}}^{\mathrm{t2}}} \tag{1}$$

and varies smoothly with decreasing temperature. As temperatures decrease a second stage in ordering occurs in which the t1 site splits into t1o and t1m sites. In practice these two processes probably proceed together and a second order parameter Q_{od} is required to monitor this further ordering behaviour. This may be defined as

$$Q_{\mathrm{od}} = \frac{X_{\mathrm{Al}}^{\mathrm{t1o}} - X_{\mathrm{Al}}^{\mathrm{t1m}}}{X_{Al}^{\mathrm{t1o}} + X_{\mathrm{Al}}^{\mathrm{t1m}}} \tag{2}$$

The thermodynamics of albite, K-feldspar and anorthite, individually, have been handled in terms of two such order parameters in Holland & Powell (1996), but not as yet together in ternary feldspars. Here, below, following Holland & Powell (1996), the order parameter definitions adopted omit the normalisations (the denominators) in equations 1 and 2, so $Q_{\rm t} = X^{\rm t1}_{\rm Al} - X^{\rm t2}_{\rm Al}$ and $Q_{\rm od} = X^{\rm t1o}_{\rm Al} - X^{\rm t1m}_{\rm Al}$.

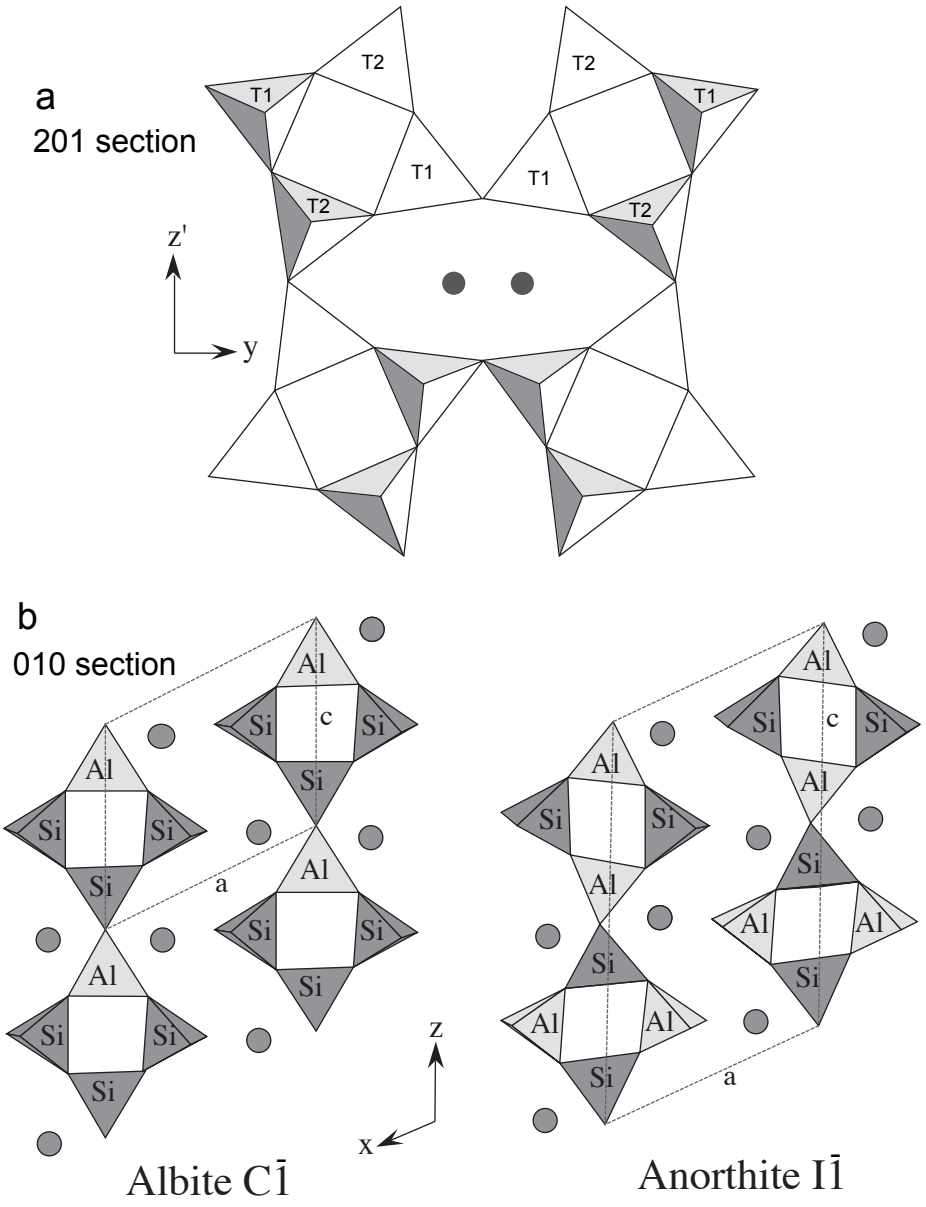

Fig. 1. Structure of feldspars illustrating the t1 and t2 tetrahedral sites and positions of the large cations Ca, Na and K (circles). (a): (201) section showing 4-member rings of t sites; (b): (010) section showing albite and anorthite ordering schemes with the unit cell a and c edges and the doubling of the c cell dimension in anorthite.

The nature of order-disorder in the plagioclase solid solution permits various phenomena that might have a significant impact on the thermodynamics of mixing. The $C\bar{1}$–$I\bar{1}$ transition appears to be first-order,

and stable between ca. 800°C and the solidus (Jin *et al.*, 2018). A model containing the $Q_{\rm t}$ and $Q_{\rm od}$ parameters should in principle be intrinsically capable of modelling the transition, although, in our "2Q" model (see below), we did not succeed in producing such a transition. Other structural phenomena seen in plagioclase are not intrinsic to a model containing $Q_{\rm t}$ and $Q_{\rm od}$, and it is not clear how they could be directly modelled. One is the strong tendency towards the reduction of Al–O–Al linkages (Al-avoidance; e.g. Kerrick & Darken, 1975), which introduces a short-range order, equating to a reduction in the configurational entropy contribution from tetrahedral-site mixing. Another is the incommensurately-ordered (aperiodic) structures taken on by intermediate-composition plagioclases, known as *e*-plagioclases, which may be stable at up to 800°C (Jin *et al.*, 2020, and references therein).

3 Thermodynamic models of feldspar

Many different simple models have been considered and fitted to the experimental database outlined above in an attempt to find one that is acceptable for real-world petrological calculations. The models cover a range of assumptions regarding the tetrahedral sites on which mixing of Si and Al occurs, and a range of behaviours relating to short-range order on those sites, relating also to the $\rm NaSi(CaAl)_{-1}$ and $\rm KSi(CaAl)_{-1}$ substitutions. The effect of short-range order is to reduce the entropic contribution to the *a*-*x* relationships. We accommodate the reduction with an empirical approach, introduced in Holland & Powell (1996), and outlined in Appendix 1 here. A model in the following list, for example 4T, becomes model 4TR when entropy reduction is invoked.

The non-ideal mixing in the *a*-*x* relationships is chosen to be via an asymmetric van Laar model with an interaction energy $W_{\rm i,j}$ for each pair of end-members and an asymmetry parameter $\alpha_{\rm i}$ for each end-member (Holland & Powell 2003).

Seven mixing models were considered for the *a*–*x* relationships. Of these models, 4, 5 and 6 in the list below were further investigated using a variety of entropy reduction factors. The seven essential structures were:

1. Simple molecular mixing. This is a fully ordered model in which all tetrahedral disorder is ignored and taken to be fixed by complete correlation with A-site Na-Ca occupancy, for example, as in Holland & Powell (2003).

2. A full ordering (2Q) model, as outlined above, involving the $Q_{\rm t}$ and $Q_{\rm od}$ order parameters.

3. 1Q model. This model can be thought of as a simplification of model 2, involving only t1–t2 ordering, implying that further t1m–t1o ordering, which is important only at more albitic compositions, may be ignored. In the case of complete order this model reduces to the 2T Al-avoidance model 4.

4. 2T model. This is the so-called Al-avoidance model of Kerrick & Darken (1975), in which Al and Si mix on only 2 of the four tetrahedral sites.

5. 4T model. This is the fully disordered plagioclase model in which complete disorder is assumed to occur on all 4 tetrahedral sites. Model 4TR is the preferred model, as discussed below.

6. Intermediate end-member model. This model involves an additional species, for example, midway between albite and anorthite, and may be formulated in a variety of ways depending on whether or not the T sites contribute to mixing.

7. Macroscopic ordering model. This involves introducing tetrahedral site ordering without specifying the sites or number of sites involved. For example, one possibility investigated involved mixing of $AlSi_3$ and Al_2Si_2 clusters on the T sites.

4 Calibration of models

Of the 7 models put forward above, models 1 and 4 were rejected on the basis of poorer fits to one or more of the main constraining datasets (cation exchange, ternary feldspar pairs, plagioclase melting loop), and models 3, 6 and 7 added complexity to calculations without providing better fits to the data. In this section we present results of the calibration of the 4TR model, along with the 2Q model for comparison, as they are two of the best-performing models. The 4TR model is our preferred model, involving complete disorder on the four T sites in feldspar, and the effect of short-range ordering approximated by reducing their entropic contribution by a factor of 4 ($\theta = 4$ in Appendix 1).

The 2Q model fully describes tetrahedral-site long-range ordering honouring the underlying order-disorder involving both the partition of Al and Si between the t1 and t2 sites, and then the partition between the t1o and t1m sites that are present when the t1 site is split. Further details of the 2Q model are provided in Appendix 2.

Calibration of the new thermodynamic models involves using (a) the plagioclase cation-exchange experiments, (b) the alkali feldspar solvus, (c) experimental ternary feldspar pairs at $880 - 900$°C, and (d) the dry melting loop for plagioclase at 1 bar. These are discussed in turn below. These data were fitted simultaneously using a Monte-Carlo approach in which pressure, temperature and feldspar compositions were calculated in THERMOCALC and filtered *via* brackets derived from the experimental studies. Model parameters were varied in the Monte-Carlo runs until 100 successful runs (those generating results within the filter brackets) were achieved (see Green *et al.*, 2016, p848, Holland *et al.*, 2018). The experimental data used in fitting for the parameters of the plagioclase and melt model discussed above are listed in tables in Appendix 3. These tables comprise 36 sets of brackets (filters) for the Monte-Carlo runs.

On the basis of the calibration shown below, the 4TR model was selected as our preferred model, even

though it is the 2Q model that explicitly represents order–disorder on the tetrahedral sites. The simplicity of the 4TR model recommends it over the 2Q model, given that its performance is no worse – indeed, somewhat better – than the 2Q model. We note that a good fit was achieved even though none of the models investigated represents the $C\bar{1}$–$I\bar{1}$ transition, or an *e*-plagioclase structure, in any way. Apparently, these structural phenomena make an insignificant energetic contribution to phase equilibria, at least by comparison with the short-range order induced by Al-avoidance.

4.1 (a) Ca-Na cation exchange experiments

Orville (1972) and Schliestedt and Johannes (1990) presented experimental details of equilibrated pairs of plagioclase feldspar and NaCl–$CaCl_2$ fluid at 2 kilobars pressure at 700°C and 600°C, and used the following exchange reaction to deduce the activities of albite and anorthite.

$$2\ \mathrm{ab} + \mathrm{CaCl_2} = \mathrm{an} + 2\ \mathrm{NaCl} + 4\ \mathrm{q}$$

Brackets (see Appendix 3) from the experimental data shown in Fig. 2 were used for calibration, together with the assumption of ideal mixing in the aqueous fluid phase ($a_{\mathrm{NaCl}} = m_{\mathrm{NaCl}}$, $a_{\mathrm{CaCl_2}} = m_{\mathrm{CaCl_2}}$). This assumption is justified *a posteriori* by the satisfactory agreement with the other experimental data for plagioclase and ternary feldspars discussed below. The results are expressed in Ca/(Ca+Na) equivalent units (i.e. 2Ca/(2Ca+Na)) as discussed in Orville (1972) in order to compare with his diagram. As may be seen in Fig. 2, the cation exchange is closely approximated by the calculated models, except for small departures at high X_{an} with the 2Q model. It should be remembered that rather few experiments are true reversals using crystalline starting compositions, and those only at Ca-poor compositions. In addition, only compositions less than $X_{\mathrm{an}} = 0.82$ were approached from both directions. Brackets from Schliestedt &

Johannes (1990) at 600°C and 2 and 5 kbar were also used in the Monte-Carlo analysis.

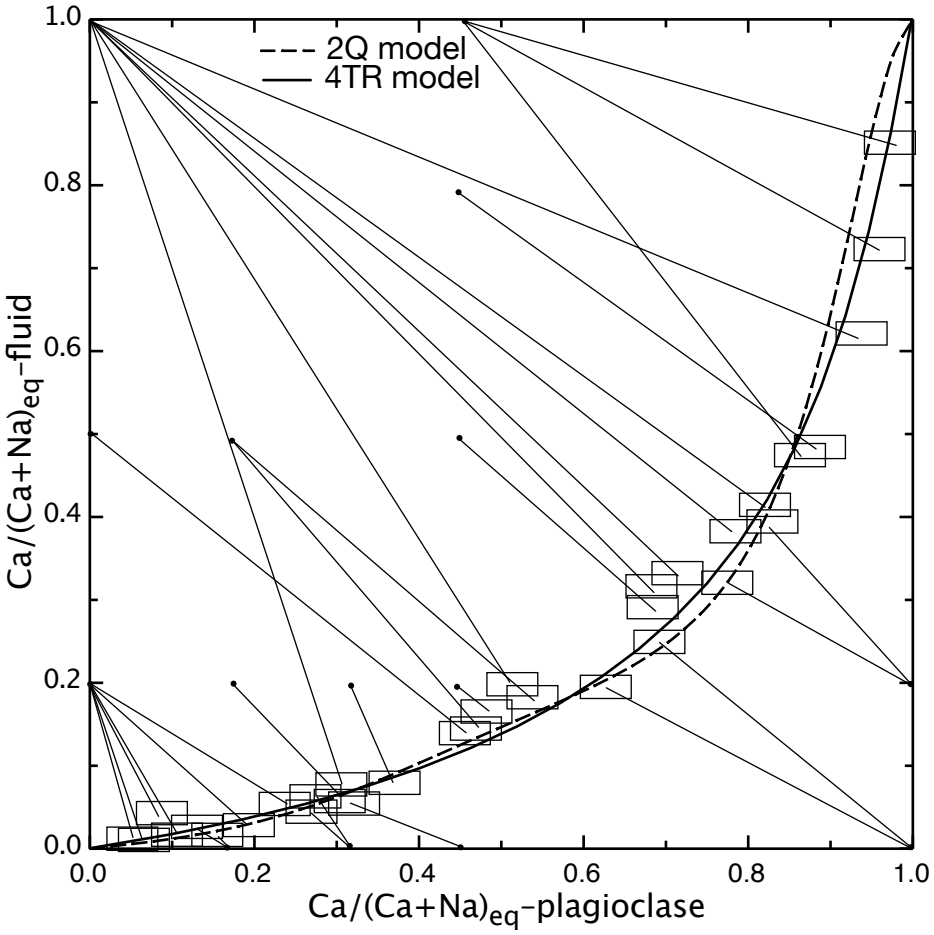

Fig. 2. Experimental Ca-Na cation-exchange data for plagioclase–fluid at 700°C (boxes, Orville 1972) and calculated curves for the 2Q and 4TR models. Thin lines join starting and final compositions. Error boxes approximated as slightly smaller than those of Schliestedt and Johannes (1990) to reflect the smaller data scatter.

The experiments of Schliestedt and Johannes (1990) are slightly more scattered and displaced to slightly higher Ca contents of plagioclase at any fluid composition (Fig. 3) than those of Orville (1972), although possibly within combined experimental uncertainties, and are slightly less consistent with all the other data fitted simultaneously in the Monte-Carlo analysis. As shown in Fig. 3 and noted by Schliestedt and Johannes (1990) their data at 2kb, 700°C, 2kb, 600°C and 5 kb, 600°C show the virtually identical

exchange behaviour. However they allow the model calibration to extend down to 600°C.

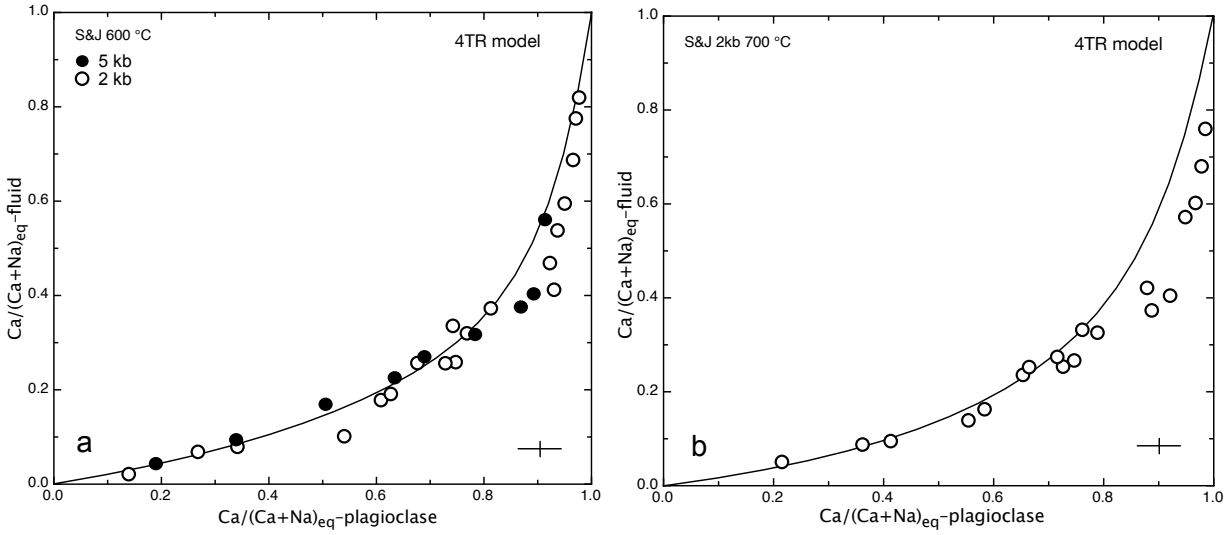

Fig. 3. Experimental Ca-Na cation-exchange data for plagioclase–fluid at 600°C (a) and at 700°C (b). Data of Schliestedt and Johannes (1990) and calculated curves for the 4TR model. Calculated curves at 2 kb and 5 kb are coincident within error. Size of error bar from Schliestedt and Johannes (1990).

4.2 (b) Alkali feldspar solvus experiments

The alkali feldspar solvus was modelled previously by Holland & Powell (2003) and the parameters used there were taken as starting points in this study. Brackets at 2 kbar and 550, 600, 650°C (Luth & Tuttle 1966, Orville 1963) and at 14-15 kbar and 500, 550, 600°C (Goldsmith & Newton 1974) were used in the Monte-Carlo runs to ensure consistency with the other experimental constraints discussed below. The fit ($W_{\mathrm{ab\ san}} = 24.1 - 0.00957T + 0.338P$ ($\pm$0.2) kJ, $\alpha_{\mathrm{ab}} = 0.674$ ($\pm$0.02), with α_{san} set at 1.0) differs slightly from that presented in Holland & Powell (2003) but the calculated solvi are almost indistinguishable from Fig. 3 in that work. In the case of the 2Q model, the calculated solvus is the same as for the 4TR model, but using the W and α values given in Appendix 3 involving the three albite end-members and disordered sanidine.

4.3 (c) Ternary feldspar equilibration experiments of Elkins & Grove (1990)

The ternary feldspar system has been investigated extensively by Ghiorso (1984), Green & Usdansky (1986), Fuhrmann & Lindsley (1988) and Elkins & Grove (1990), using the Margules formulation for mixing energetics. Elkins & Grove (1990) analyzed their experimental results in the range 700–900°C with a one-site entropy of mixing and a subregular solution. In Holland & Powell (2003) the solution model also used a one-site entropy of mixing model in demonstrating the applicability of the van Laar and DQF

approach, whereas we here use a reduced-entropy tetrahedral site model as described above.

The four experimental tie line pairs shown joining the grey composition regions in Fig. 4 (at 1 kbar and around 900°C) were taken in the Monte-Carlo fitting, together with pairs at 1 and 2 kbar at 800°C. As may be seen, for the 4TR model the calculated tie lines are slightly less steep at high Ca contents than implied by the experimental data, although it should be noted that the earlier work of Seck (1971) has slopes similar to the 4TR calculated ones. The 2Q model performs somewhat less well than that 4TR model, yielding still less steep tielines.

The 4TR model plagioclase solid solution parameters are

$$
\begin{aligned}
W_{\mathrm{ab\,an}} &= 14.6 - 0.00935T - 0.04P\ (\pm 0.3)\ \mathrm{kJ} \\
W_{\mathrm{ab\,or}} &= 24.1 - 0.00957T + 0.338P\ (\pm 0.2)\ \mathrm{kJ} \\
W_{\mathrm{an\,or}} &= 48.5 - 0.13P\ (\pm 0.5)\ \mathrm{kJ}
\end{aligned}
$$

$$
\begin{aligned}
\alpha_{\mathrm{ab}} &= 0.674\ (\pm 0.002) \\
\alpha_{\mathrm{an}} &= 0.550\ (\pm 0.003) \\
\alpha_{\mathrm{or}} &= 1.00\ (\mathrm{fixed})
\end{aligned}
$$

The uncertainties given above are just those that come from the ranges consistent with the filters in the Monte-Carlo fitting. They represent merely a guide to likely magnitudes, in the context of the essentially unquantifiable underlying model assumptions.

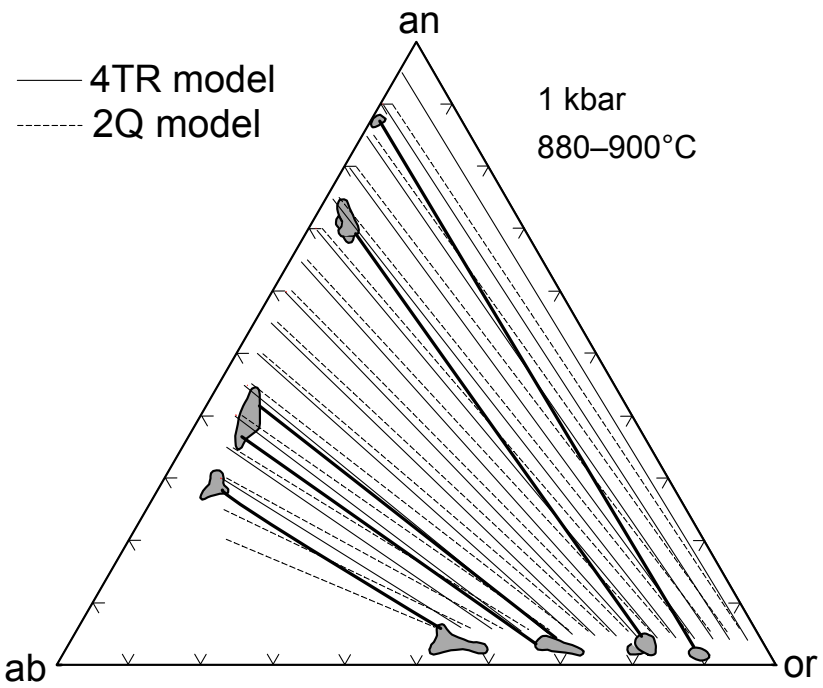

Fig. 4. Ternary feldspar relations at 1 kbar and 880–900°C. Grey fields are experimental plagioclase–K-feldspar pairs with tie lines (heavy lines) from Elkins & Grove (1990). Tie lines joining plagioclase and K-feldspar (light lines) are calculated.

4.4 (d) Binary plagioclase melting at 1 bar of Bowen (1913)

Experimental data from Bowen (1913) on binary plagioclase melting were also used in the Monte-Carlo analysis as additional constraints on the model. Pairs of coexisting plagioclase and melt at 1120, 1200, 1300, 1400, 1500 and 1552°C were used as constraints. To ensure correct melting temperatures for pure albite and pure anorthite, Gibbs free energy increment parameters ($\Delta G^{\rm mod}_{\rm anL}$ and $\Delta G^{\rm mod}_{\rm abL}$) were also determined along with a symmetric (regular solution) mixing parameter ($W_{\rm anL\ abL}$) for melt.

The calculated melting loop is shown in Fig. 5 compared with the experiments of Bowen (1913). The agreement is good for both liquid and plagioclase compositions, especially considering the difficulties of equilibration in dry feldspar melting experiments, and hence in obtaining appropriate plagioclase compositions (Johannes *et al.* 1994). The performance of the 4TR model is marginally better than that of the 2Q model.

The abL–anL melt mixing parameters are

$$
\begin{aligned}
W_{\rm anL\ abL} &= 2.2\ (\pm 0.2)\ {\rm kJ} \\
\Delta G^{\rm mod}_{\rm abL} &= -0.15\ (\pm 0.2)\ {\rm kJ} \\
\Delta G^{\rm mod}_{\rm anL} &= 0.50\ (\pm 0.2)\ {\rm kJ}
\end{aligned}
$$

As in the earlier work of Holland & Powell (2001) anorthite–albite melt is found to be a nearly ideal solution.

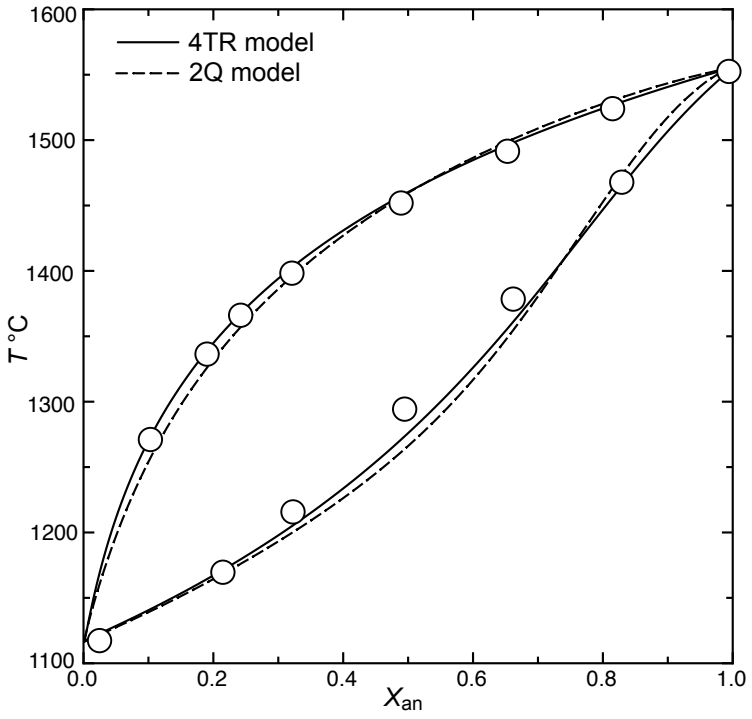

Fig. 5. Plagioclase melting loop at 1 bar. Circles are experimental results of Bowen (1913). Curves are calculated with the 4TR and 2Q models.

5 Testing and application of the 4TR model

The 4TR model described and calibrated above is consistent with a wide range of experimental data over a range in temperature from 600–1550°C, suggesting that this entropy model and associated non-ideal mixing terms is appropriate for calculations for a wide range in rock formation conditions. We have left two experimental studies from our fitting in order to provide a check on the consistency of the model. The studies involve calorimetric data on enthalpy of mixing in plagioclase and displaced-activity phase equilibrium experiments involving plagioclase at high pressures.

Newton *et al.* (1980) and Carpenter *et al.* (1985) provide enthalpy of solution data for plagioclases equilibrated at high temperatures (1100–1400°C) and run in a high-temper- ature solution calorimeter at 970K. As a test of the 4TR model we present a comparison of the calculated enthalpy of solution in Fig. 6 where the model compares favourably with the calorimetric data within its relatively large scatter. There appears to be slightly better agreement with the Newton *et al.* (1980) data perhaps because the model and their calorimetry are both based on synthetic plagioclases.

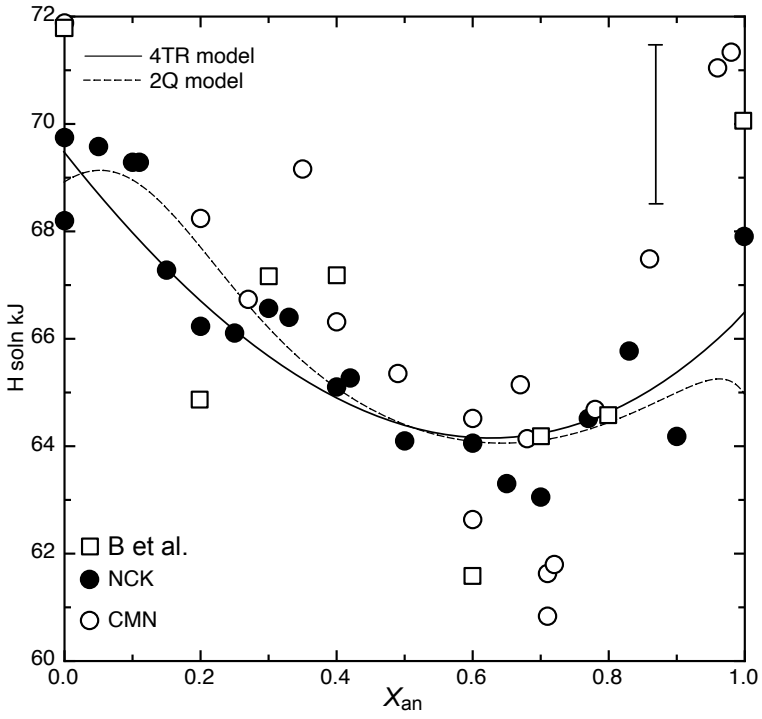

Fig. 6. Plagioclase enthalpy of solution data from Newton *et al.* (1980), shown as black circles and the calculated 4TR and 2Q model curves for comparison. Open circles are heat-treated samples of Carpenter *et al.* (1985). Open squares are data of Benisek et al. (2003). Calculated values for albite and anorthite are arbitrarily taken as 69.5 and 66.5 kJ respectively. Vertical bar shows average error for experimental points.

As a final test, the experimental data of Windom & Boettcher (1976) on plagioclases equilibrated with

wollastonite + grossular + quartz at 1100°C are compared with the 4TR model calculation. Figure 6 shows the experimental pressure brackets with the 4TR model providing a reasonable fit to the experimental data. In Fig. 7 the experimental pressures have been adjusted by -0.7 kbar such that the pressure for pure an + wo = gr + q agrees with Windom & Boettcher's brackets, because the Holland & Powell (2011) dataset yields a pressure of 14 kbar at that temperature. This corresponds to a 5% friction correction and is typical of those applied to piston-cylinder experiments. The good agreement with the plagioclase trend in $X_{\rm an}$ from 0.3 to 1.0 at pressures of 15–20 kbar suggest that the plagioclase model is reliable through the pressure range of plagioclase stability.

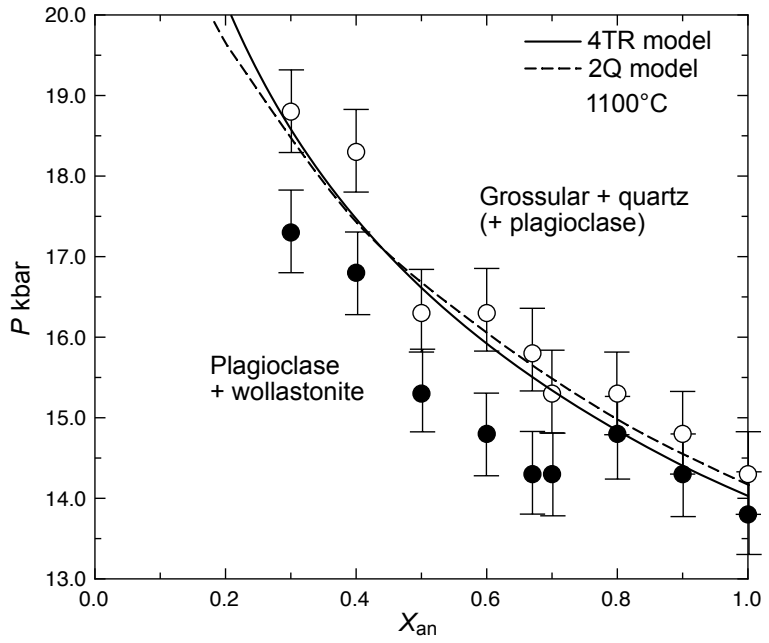

Fig. 7 Experimental determination of plagioclase compositions coexisting with grossular, wollastonite & quartz from Windom & Boettcher (1976). Circles with error bars are experimental brackets, and the curves are calculated with the 4TR and 2Q models.

The 4TR (and the 2Q) model predict increasing non-ideality with decreasing temperature, which, at low temperatures, leads to a miscibility gap which closes at about 260°C and widens to lower temperature (Fig. 8). It is not meaningful to compare this calculated gap with either the Hüttenlocher or Bøggild gaps, as neither any stable regions of *e*-plagioclase nor the C$\bar{1}$–I$\bar{1}$ transition have been taken into account here.

In metabasic systems in particular, the peristerite gap is an important feature, especially in the greenschist to amphibolite facies transition. In order to simulate a peristerite gap, we introduce a low albite feldspar with properties that yield a narrow peristerite-like gap at very low $X_{\rm an}$ and which closes at around 600°C (e.g. Carpenter 1981, Nord *et al.* 1978). The mixing properties of the low albite solid solution involve a simple 1-site entropy of mixing and the parameters below. These generate a first order transition

at 600°C and the miscibility gap shown in Fig. 8, and considerably widen the miscibility gap between albite and plagioclase at low temperatures. As discussed in Nord *et al.* (1978) and Starr and Pattison (2019), whether the miscibility gap is a solvus or a binary loop is unresolved; our model assumes the latter.

$$
\begin{aligned}
W_{\text{an ab}} &= 3.4\ (\pm 0.3)\ \text{kJ} \\
\alpha_{\text{an}} &= 1.00\ \text{(fixed)} \\
\alpha_{\text{ab}} &= 0.64\ (\pm 0.02) \\
\Delta G^{\text{mod}}_{\text{ab}} &= -1.746 + 0.002T\ (\pm 0.05)\ \text{kJ} \\
\Delta G^{\text{mod}}_{\text{an}} &= 10.00\ (\pm 0.05)\ \text{kJ}
\end{aligned}
$$

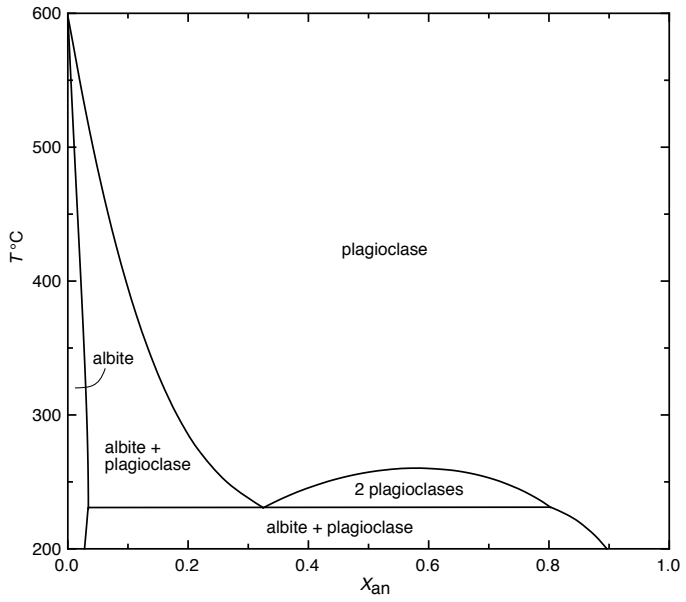

Fig. 8. Calculated T–X_{an} section, showing the miscibility gap below around 260°C and the model peristerite gap at very low X_{an} separating almost pure albite from an-rich plagioclase at lower temperature.

The calculated solvus relations below 300°C, even if predicted correctly, are metastable with respect to *e*-plagioclase and the phase relationships associated with the Hüttenlocher and Bøggild gaps.

A simple example of the application of the feldspar model is to investigate the melting relationships of quartzofeldspathic rocks in the absence of H_2O. Given the difficulty of determining metamorphic temperatures for UHT rocks, the dry melting relationships provide an effective upper temperature limit of crustal metamorphism, considered in terms of the metamorphism of broadly granitic rocks. Calculations in the system CaO-Na_2O-K_2O-Al_2O_3-SiO_2, with quartz and sillimanite in excess, can be projected onto the ternary feldpar compatibility diagram, ab–an–or. Dry melting in ab-or starts at an azeotropic point at 1105°C and then spreads rapidly into the interior of the ternary feldspar triangle. By 1108°C there is a pl-ksp-liq tie triangle. With temperature increase, this tie triangle swings up and across towards the an–or

side of the diagram (Fig. 9a). This shows that for normal granitic crustal compositions the upper limit of crustal metamorphic temperatures is 1100°C. Figure 9b shows the phase relationships at 1110°C. In the presence of even a small amount of H_2O in the bulk composition of a granitic rock, melting will occur at markedly lower temperature than 1100°C. For example, at $a_{H_2O} = 0.05$, the equivalent position of the pl-ksp-liq tie triangle in (b) is 1025°C.

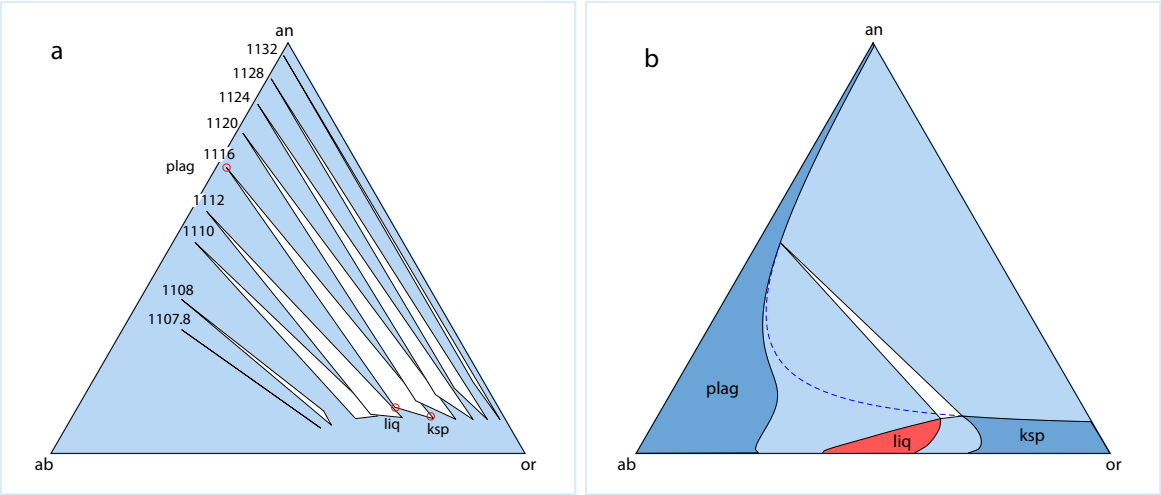

Fig. 9. The 4TR model ternary diagrams, with excess sillimanite and quartz, at 8 kbar. (a) Migration of the 2-feldspar + liquid triangle with temperature (in °C). The lowest temperature "tie trangle", essentially a colinear relationship between the phases, marks the temperature at which liq breaks through the feldspar one-phase field into the body of the ab-an-or triangle, via a singular reaction. The positions of plag, liq and ksp at 1116°C are highlighted to show relative locations. (b) Showing phase relations of feldspars and liquid at 1110°C.

6 Discussion and Conclusions

Although the full order-disorder 2Q model is shown to be in reasonable agreement with experimental constraints, the simpler 4TR model can satisfy them as well, if not better. Both models omit the C$\bar{1}$–I$\bar{1}$ transition, and the presence of intermediate-composition *e*-plagioclase (whether stable or metastable). However, there is no clear evidence in calibration data that these phenomena significantly affect the results of the lower-temperature experiments. They appear to have only small consequences for the thermodynamics of the solid solution.

The plagioclase a–x relations of Holland & Powell (1992) explicitly represented the C$\bar{1}$–I$\bar{1}$ transition, by having a separate thermodynamic model for each structure, Given that at least above 800°C, the C$\bar{1}$–I$\bar{1}$ transition is a line in a T-x diagram (not a 2-phase field), the separate thermodynamic models were made to be contiguous at the transition. Holland & Powell (2003) extended this approach into the ternary feldspar system. We now realise that it is not possible to make this extension into ternary feldspars without

breaking the contiguity constraints, resulting in complex coexisting feldspar relations as an unwanted artefact. The new 4TR feldspar model can be seen as a replacement for the Holland & Powell (2003) model, which appropriately if implicitly represents the entropic consequences of configurational order-disorder. Like its predecessor, it is suitable for use in petrological phase equilibrium calculations along with version 6 of the Holland & Powell dataset (Holland & Powell, 2011), and associated families of activity-composition relations (White *et al.*, 2014; Green *et al.*, 2016; Holland *et al.*, 2018). The new plagioclase model should produce results that differ inconsequentially from the earlier models, but obviates the need to decide on whether the calculated plagioclase is C$\bar{1}$ or I$\bar{1}$ and removes any small disconnects or artificial C$\bar{1}$–I$\bar{1}$ coexisting feldspar pairs. The plagioclase of Tomlinson & Holland (2021) is based on model 6 of this study and, while it should produce similar results, the new 4TR model presented here is recommended.

Acknowledgements

We thank Richard White for conversations about activity-composition relations, and the reviewers, Nicolas Riel and Jacob Forshaw, for their helpful comments and suggestions.

References

Benisek, A., Kroll, H., Cemic,L., Kohl,V., Breit, U. & Heying, B. 2003. Enthalpies in (Na,Ca)- and (K,Ca)-feldspar binaries: a high-temperature solution calorimetric study. *Contributions to Mineralogy and Petrology, 145*, 119–129.

Benisek, A., Dachs, E. & Kroll, H. 2010. A ternary feldspar-mixing model based on calorimetric data: development and application. *Contributions to Mineralogy and Petrology, 160*, 327–337.

Bowen, N.L. 1913. The melting phenomena of the plagioclase feldspars. *American Journal of Science, 35(210)*, 577–599.

Carpenter M.A. 198l. A "conditional spinodal" within the peristerite miscibility gap of plagioclase feldspars. *American Mineralogist, 66*, 553–560.

Carpenter, M.A. & McConnell, J.D.C. 1984. Experimental delineation of the $C\bar{1}$–$I\bar{1}$ transformation in intermediate plagioclase feldspars. *American Mineralogist, 69*, 112–121.

Carpenter, M.A., & Salje, E.K.H 1994. Thermodynamics of nonconvergent cation ordering in minerals: III. Order parameter coupling in potassium feldspar. *American Mineralogist, 79*, 1084–1098

Carpenter, M.A., McConnell, J.D.C. & Navrotsky, A. 1985. Enthalpies of ordering in the plagioclase feldspar solid solution. *Geochimica et Cosmochimica Acta, 49*, 947–966.

Carpenter, M.A. 1994. Subsolidus phase-relations of the plagioclase feldspar solid-solution. In: Ian Parsons (Ed.) *Feldspars and their reactions.* Springer, Dordrecht, pp 221–269.

Elkins, L.T. & Grove, T.L. 1990. Ternary feldspar experiments and thermodynamic models. *American Mineralogist, 75*, 544–559.

Fuhrman, M.L. & Lindsley, D.H. 1988. Ternary feldspar modeling and thermometry. *American Mineralogist, 73*, 201–215.

Ghiorso, M.S. 1984. Activity/composition relations in the ternary feldspars. *Contributions to Mineralogy and Petrology, 87*, 282–296

Goldsmith J.R & Newton R.C. 1974. An experimental determination of the alkali feldspar solvus. In: The Feldspars (ed WS MacKenzie & J Zussman). Manchester University Press.

Green, N.L. & Usdansky, S.T. 1986. Ternary feldspar relations and feldspar thermobarometry. *American Mineralogist, 71*, 1100–1108.

Green, E.C.R., White, R.W., Diener, J.F.A., Powell, R., Holland, T.J.B. & Palin, R.M. 2016. Activity?composition relations for the calculation of partial melting equilibria in metabasic rocks. *Journal of Metamorphic Geology*, 34, 845–869.

Holland T.J.B. & Powell R. 1992. Plagioclase feldspars: activity-composition relations based upon Darken's quadratic formalism and Landau theory. *American Mineralogist, 77*, 53–61

Holland, T. J. B. & Powell, R. 1996. Thermodynamics of order-disorder in minerals: 1. Symmetric formalism applied to minerals of fixed composition. *American Mineralogist, 81*, 1413–1424.

Holland, T.J.B., & Powell, R. 1998. An internally-consistent thermodynamic dataset for phases of petrological interest. *Journal of Metamorphic Geology, 16*, 309–344.

Holland, T. J. B. & Powell, R. 2001. Calculation of phase relations involving haplogranitic melts using an internally-consistent thermodynamic dataset. *Journal of Petrology, 42*, 673–683.

Holland, T.J.B., & Powell, R. 2003. Activity–composition relations for phases in petrological calculations: an asymmetric multicomponent formulation. *Contributions to Mineralogy and Petrology, 145*, 492–501.

Holland, T.J.B. & Powell, R. 2011. An improved and extended internally consistent thermodynamic dataset for phases of petrological interest, involving a new equation of state for solids. *Journal of Metamorphic Geology, 29*, 333–383.

Holland, T.J., Green, E.C.R. & Powell, R. 2018. Melting of peridotites through to granites: a simple thermodynamic model in the system KNCFMASHTOCr. *Journal of Petrology*, 59, 881–900.

Jin, S. & Xu, H. 2017. Investigations of the phase relations among e1, e2 and C$\bar{1}$ structures of Na-rich plagioclase feldspars: a single-crystal X-ray diffraction study. *Acta Crystallographica Section B: Structural Science, Crystal Engineering and Materials*, 73, 992–1006.

Jin, S., Wang, X. & Xu, H. 2018. Revisiting the I$\bar{1}$ structures of high-temperature Ca-rich plagioclase feldspar–a single-crystal neutron and X-ray diffraction study. *Acta Crystallographica Section B: Structural Science, Crystal Engineering and Materials*, 74, 152–164.

Jin, S., Xu, H., Wang, X., Zhang, D., Jacobs, R. & Morgan, D. 2019. The incommensurately modulated structures of volcanic plagioclase: displacement, ordering and phase transition. *Acta Crystallographica Section B: Structural Science, Crystal Engineering and Materials*, 75, 643–656.

Jin, S., Xu, H., Wang, X., Zhang, D., Jacobs, R. & Morgan, D. 2020. The incommensurately modulated structures of low-temperature labradorite feldspars: a single-crystal X-ray and neutron diffraction study. *Acta Crystallographica Section B: Structural Science, Crystal Engineering and Materials*, 76, 93–107.

Johannes, W. Koepke, J. & Behrens, H. 1994. Partial Melting Reactions of Plagioclases and Plagioclase-Bearing Systems. In Feldspars and Their Reactions (Ed: lan Parsons). Springer, Dordrecht, Netherlands 161–194.

Kerrick, D.M. & Darken, L.S. 1975. Statistical thermodynamic models for ideal oxide and silicate solid solutions, with applications to plagioclase. *Geochimica et Cosmochimica Acta, 39*, 1431-1442.

Luth, W.C. & Tuttle O.F. 1966 The alkali feldspar solvus in the system Na_2O–K_2O–Al_2O_3–SiO_2–H_2O. *American Mineralogist, 51*, 1359–1373.

McConnell, J.D.C. 2008. The origin and characteristics of the incommensurate structures in the plagioclase feldspars. *The Canadian Mineralogist* 46, 1389–1400.

Newton, R.C., Charlu, T.V. & Kleppa, O.J. 1980. Thermochemistry of the high structural state plagioclases. *Geochimica et Cosmochimica Acta, 44*, 933–941.

Nord, G. L., Jr., Hammarstrom, J. L., & Zen, E-An. 1978. Zoned plagioclase and peristerite formation in phyllites from south-western Massachusetts. *American Mineralogist, 63*, 947–955.

Orville, P.M. 1963. Alkali ion exchange between vapor and feldspar phases. *American Journal of Science, 261*, 201–237.

Orville, P.M. 1972. Plagioclase cation exchange equilibria with aqueous chloride solution: results at 700°C and 200 bars in the presence of quartz. *American Journal of Science, 272*, 234–272.

Schliestedt, M. & Johannes, W. 1990. Cation exchange equilibria between plagioclase and aqueous chloride solution at 600 to 700°C and 2 to 5 kbar. *European Journal of Mineralogy, 2*, 283–295.

Seck, H.A. (1971). Koexistierende Alkalifeldspäte und Plagioklase im System NaAlSi3O8-KAlSi3O8-CaAl2Si2O8-H2O bei Temperaturen von 650°C bis 900°C. *N Jahrb Mineral Abhand* **115**, 315–342

Starr, P.G. & Pattison, D.R.M. 2019. Equilibrium and disequilibrium processes across the greenschist–amphibolite transition zone in metabasites. *Contributions to Mineralogy and Petrology, 174*, 1–18.

Tomlinson, E.L. & Holland, T.J.B. 2021. A Thermodynamic Model for the Subsolidus Evolution and Melting of Peridotite. *Journal of Petrology, 62*, 1–23.

White, R.W., Powell, R., Holland, T.J.B., Johnson, T.E. & Green, E.C.R. 2014. New mineral activity?composition relations for thermodynamic calculations in metapelitic systems. *Journal of Metamorphic Geology*, 32, 261–286.

Windom, K.E. & Boettcher, A.L. 1976. The effect of reduced activity of anorthite on the reaction grossular + quartz = anorthite + wollastonite: a model for plagioclase in the earth's lower crust and upper mantle. *American Mineralogist, 61*, 889–896.

Appendix 1: Simulation of short-range ordering

The reduction of the entropy of mixing to simulate the effect of local, or short-range, ordering is an empirical device introduced in Holland & Powell (1996) for spinel Mg-Al ordering and Holland & Powell (1998) for amphiboles, and has been used widely in a-x modelling since then, e.g. White *et al.* (2014). Such entropy reduction is illustrated here using the 2T and 4T models (see text) for plagioclase. First, for the 2T model

$$\begin{aligned} a_{\rm an}^{\rm ideal} &= x_{\rm Ca,A}\,(x_{\rm Al,TB}^{2}) \\ a_{\rm ab}^{\rm ideal} &= 4^{\frac{1}{\theta}}\,x_{\rm Na,A}\,(x_{\rm Al,TB}\,x_{\rm Si,TB}) \end{aligned}$$

Now consider a 2TR model (R meaning reduced entropic contribution), with the entropic contribution of the tetrahedral sites to be reduced by a factor, θ. With $\theta > 1$, this amounts to asserting that the NaSi(CaAl)$_{-1}$ coupled substitution exerts an additional short-range effect, on top of that provided by Al avoidance.

$$\begin{aligned} a_{\rm an}^{\rm ideal} &= x_{\rm Ca,A}\,(x_{\rm Al,TB}^{2})^{\frac{1}{\theta}} \\ a_{\rm ab}^{\rm ideal} &= 4^{\frac{1}{\theta}}\,x_{\rm Na,A}\,(x_{\rm Al,TB}\,x_{\rm Si,TB})^{\frac{1}{\theta}} \end{aligned}$$

In these expressions the TB sites are the sites that admit Al and Si and the pre-factor for ab is a normalisation constant. In the simple 2T (or Al-avoidance) model, $\theta = 1$. If θ is large the ideal mixing activities reduce to those of molecular mixing, as used in Holland & Powell (2003), with $a_{\rm an}^{\rm ideal} = x_{\rm Ca,A}$, $a_{\rm ab}^{\rm ideal} = x_{\rm Na,A}$, and $a_{\rm san}^{\rm ideal} = x_{\rm K,A}$. The magnitude of θ for any model to successfully explain the experimental data is related to the entropy of mixing in the model.

For the 4T model

$$\begin{aligned} a_{\rm ab}^{\rm ideal} &= (\tfrac{256}{27})\,x_{\rm Na,A}\,(x_{\rm Al,T}\,x_{\rm Si,T}^{3}) \\ a_{\rm an}^{\rm ideal} &= x_{\rm Ca,A}\,(x_{\rm Al,T}^{2}\,x_{\rm Si,T}^{2}) \end{aligned}$$

Now consider a 4TR model, with the entropic contribution of the tetrahedral sites to be reduced by a factor, θ. The ideal mixing activities are then:

$$\begin{aligned} a_{\rm ab}^{\rm ideal} &= (\tfrac{256}{27})^{\frac{1}{\theta}}\,x_{\rm Na,A}\,(x_{\rm Al,T}\,x_{\rm Si,T}^{3})^{\frac{1}{\theta}} \\ a_{\rm an}^{\rm ideal} &= x_{\rm Ca,A}\,(x_{\rm Al,T}^{2}\,x_{\rm Si,T}^{2})^{\frac{1}{\theta}} \end{aligned}$$

As noted in the text, the 4TR model is the only one that fits all of the experimental constraints well, and involves complete disorder on the four T sites in feldspar (see text) and with $\theta = 4$. Then, the ideal mixing

activities for ab, an and or are:

$$
\begin{aligned}
a_{\mathrm{ab}}^{\mathrm{ideal}} &= (\tfrac{256}{27})^{\frac{1}{4}}\; x_{\mathrm{Na,A}}\,(x_{\mathrm{Al,T}}\,x_{\mathrm{Si,T}}^{3})^{\frac{1}{4}} \\
a_{\mathrm{or}}^{\mathrm{ideal}} &= (\tfrac{256}{27})^{\frac{1}{4}}\; x_{\mathrm{K,A}}\,(x_{\mathrm{Al,T}}\,x_{\mathrm{Si,T}}^{3})^{\frac{1}{4}} \\
a_{\mathrm{an}}^{\mathrm{ideal}} &= x_{\mathrm{Ca,A}}\,(x_{\mathrm{Al,T}}^{2}\,x_{\mathrm{Si,T}}^{2})^{\frac{1}{4}}
\end{aligned}
$$

Appendix 2: The 2Q model

The end-members used, in terms of the A, t1o, t1m and t2 sites in the 2Q model, are

	A			t1o		t1m		t2	
	Na	Ca	K	Al	Si	Al	Si	Al	Si
oab	1	0	0	1	0	0	1	0	2
dab	1	0	0	1/4	3/4	1/4	3/4	1/2	3/2
oan	0	1	0	1	0	1	0	0	2
tab	1	0	0	1/2	1/2	1/2	1/2	0	2
san	0	0	1	1/4	3/4	1/4	3/4	1/2	3/2

where oab and dab are ordered and disordered albite, tab is t1-t2 ordered albite, oan is ordered anorthite, and san is disordered sanidine. With the 4 independent variables

$$
\begin{aligned}
x &= X^{\mathrm{A}}_{\mathrm{Ca}} \\
k &= X^{\mathrm{A}}_{\mathrm{K}} \\
Q_{\mathrm{t}} &= \frac{X^{\mathrm{t1o}}_{\mathrm{Al}} + X^{\mathrm{t1m}}_{\mathrm{Al}}}{2} - X^{\mathrm{t2}}_{\mathrm{Al}} \\
Q_{\mathrm{od}} &= X^{\mathrm{t1o}}_{\mathrm{Al}} - X^{\mathrm{t1m}}_{\mathrm{Al}}
\end{aligned}
$$

Note that these expressions for the order parameters are different from those of Carpenter & Salje (1994) in equations 1 and 2 in that the normalisation in the denominators is missing, as noted in the text. This difference is not relevant to the thermodynamic analysis.

and site fractions

$$
\begin{aligned}
X^{\mathrm{A}}_{\mathrm{Na}} &= 1 - k - x \\
X^{\mathrm{A}}_{\mathrm{Ca}} &= x \\
X^{\mathrm{A}}_{\mathrm{K}} &= k
\end{aligned}
$$

$$
\begin{aligned}
X^{\mathrm{t1o}}_{\mathrm{Al}} &= \tfrac{1}{4} + \tfrac{1}{2}Q_{\mathrm{od}} + \tfrac{1}{2}Q_{\mathrm{t}} + \tfrac{1}{4}x \\
X^{\mathrm{t1o}}_{\mathrm{Si}} &= \tfrac{3}{4} - \tfrac{1}{2}Q_{\mathrm{od}} - \tfrac{1}{2}Q_{\mathrm{t}} - \tfrac{1}{4}x \\
X^{\mathrm{t1m}}_{\mathrm{Al}} &= \tfrac{1}{4} - \tfrac{1}{2}Q_{\mathrm{od}} + \tfrac{1}{2}Q_{\mathrm{t}} + \tfrac{1}{4}x \\
X^{\mathrm{t1m}}_{\mathrm{Si}} &= \tfrac{3}{4} + \tfrac{1}{2}Q_{\mathrm{od}} - \tfrac{1}{2}Q_{\mathrm{t}} - \tfrac{1}{4}x \\
X^{\mathrm{t2}}_{\mathrm{Al}} &= \tfrac{1}{4} - \tfrac{1}{2}Q_{\mathrm{t}} + \tfrac{1}{4}x \\
X^{\mathrm{t2}}_{\mathrm{Si}} &= \tfrac{3}{4} + \tfrac{1}{2}Q_{\mathrm{t}} - \tfrac{1}{4}x
\end{aligned}
$$

and end-member proportions $p_{\mathrm{oab}} = Q_{\mathrm{od}}$, $p_{\mathrm{dab}} = 1 - k + x - Q_{\mathrm{t}}$, $p_{\mathrm{oan}} = x$, $p_{\mathrm{tab}} = -Q_{\mathrm{od}} + Q_{\mathrm{t}} - 2x$, $p_{\mathrm{san}} = k$

and ideal mixing activities

$$
\begin{aligned}
a_{\mathrm{oab}} &= X^{\mathrm{A}}_{\mathrm{Na}} X^{\mathrm{t1o}}_{\mathrm{Al}} X^{\mathrm{t1m}}_{\mathrm{Si}} (X^{\mathrm{t2}}_{\mathrm{Si}})^2 \\
a_{\mathrm{dab}} &= \tfrac{256}{27} X^{\mathrm{A}}_{\mathrm{Na}} (X^{\mathrm{t1o}}_{\mathrm{Al}})^{\frac{1}{4}} (X^{\mathrm{t1o}}_{\mathrm{Si}})^{\frac{3}{4}} (X^{\mathrm{t1m}}_{\mathrm{Al}})^{\frac{1}{4}} (X^{\mathrm{t1m}}_{\mathrm{Si}})^{\frac{3}{4}} (X^{\mathrm{t2}}_{\mathrm{Al}})^{\frac{1}{2}} (X^{\mathrm{t2}}_{\mathrm{Si}})^{\frac{3}{2}} \\
a_{\mathrm{oan}} &= X^{\mathrm{A}}_{\mathrm{Ca}} X^{\mathrm{t1o}}_{\mathrm{Al}} X^{\mathrm{t1m}}_{\mathrm{Al}} (X^{\mathrm{t2}}_{\mathrm{Si}})^2 \\
a_{\mathrm{tab}} &= 4 X^{\mathrm{A}}_{\mathrm{Na}} (X^{\mathrm{t1o}}_{\mathrm{Al}})^{\frac{1}{2}} (X^{\mathrm{t1o}}_{\mathrm{Si}})^{\frac{1}{2}} (X^{\mathrm{t1m}}_{\mathrm{Al}})^{\frac{1}{2}} (X^{\mathrm{t1m}}_{\mathrm{Si}})^{\frac{1}{2}} (X^{\mathrm{t2}}_{\mathrm{Si}})^2 \\
a_{\mathrm{san}} &= \tfrac{256}{27} X^{\mathrm{A}}_{\mathrm{K}} (X^{\mathrm{t1o}}_{\mathrm{Al}})^{\frac{1}{4}} (X^{\mathrm{t1o}}_{\mathrm{Si}})^{\frac{3}{4}} (X^{\mathrm{t1m}}_{\mathrm{Al}})^{\frac{1}{4}} (X^{\mathrm{t1m}}_{\mathrm{Si}})^{\frac{3}{4}} (X^{\mathrm{t2}}_{\mathrm{Al}})^{\frac{1}{2}} (X^{\mathrm{t2}}_{\mathrm{Si}})^{\frac{3}{2}}
\end{aligned}
$$

and non-ideal mixing terms via van Laar model (in kJ)

$$
\begin{aligned}
W(\mathrm{oab}, \mathrm{dab}) &= 11 + 0.04P \\
W(\mathrm{oab}, \mathrm{oan}) &= 19.2 + 0.35P \\
W(\mathrm{oab}, \mathrm{tab}) &= 5.4 + 0.04P \\
W(\mathrm{oab}, \mathrm{san}) &= 30.4 + 0.365P \\
W(\mathrm{dab}, \mathrm{oan}) &= 40.8 + 0.34P \\
W(\mathrm{dab}, \mathrm{tab}) &= 0.6 + 0.04P \\
W(\mathrm{dab}, \mathrm{san}) &= 12.2 + 0.365P \\
W(\mathrm{oan}, \mathrm{tab}) &= 8 + 0.27P \\
W(\mathrm{oan}, \mathrm{san}) &= 77.1 - 0.093P \\
W(\mathrm{tab}, \mathrm{san}) &= 14.4 + 0.365P
\end{aligned}
$$

and the Gibbs energies of the end-members are taken to be: san = sanidine, oab = ordered albite, oan = ordered anorthite, tab = ordered albite $+15.17 - 0.011526T + 0.04P$ (kJ), dab = ordered albite $+18.12 - 0.018702T + 0.04P$ (kJ). Asymmetry parameters are: $\alpha(\mathrm{san}) = 1.00$, $\alpha(\mathrm{oan}) = 0.667$, $\alpha(\mathrm{oab}) = \alpha(\mathrm{dab}) = \alpha(\mathrm{tab}) = 0.685$.

In the 2Q model there are two internal equilibria that need to be solved to determine the state of order—Q_{t} and Q_{od}—for any composition of feldspar. These internal equilibria are $\Delta\mu = 0$ equations for each of the independent reactions between the end-members, for example, oab=dab and oab=tab. Figure A2.1 shows the variation of Q_{t} and Q_{od} at 600°C in plagioclase, solving the internal equilibria, and using the parameters listed above. At high anorthite contents, the feldspar is almost completely ordered onto the t1 and t2 sites with no ordering onto the t1o and t1 m sites, while at albitic compositions the t1 and t2 are approximately half ordered and there is a high degree of ordering onto the to1 and t1m sites, as expected.

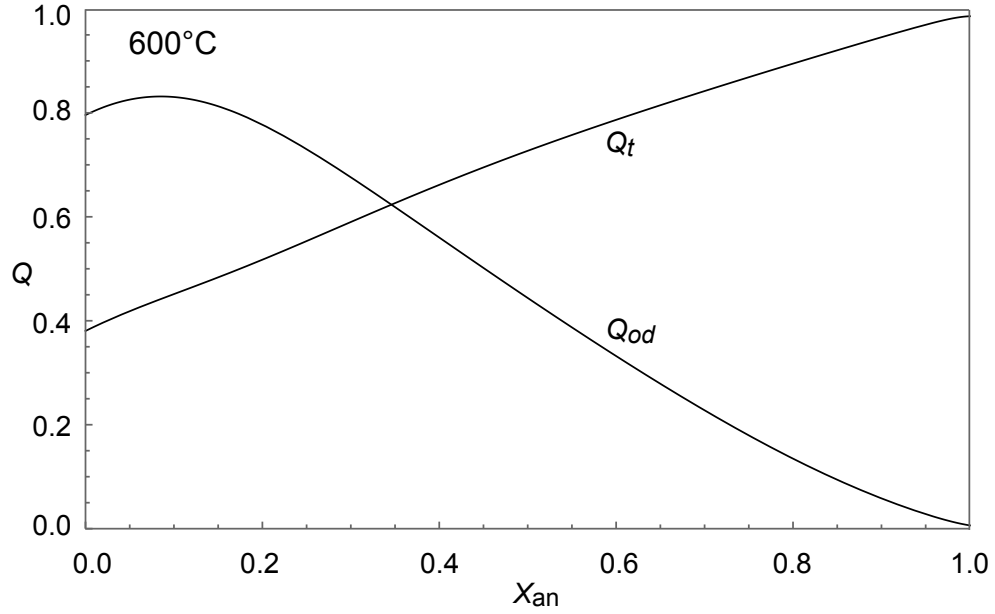

Fig. A2.1. Calculated variation of Q_{t} and Q_{od} with plagioclase composition at 600°C for the 2Q model.

Appendix 3: Data used in fitting

1. Orville (1972) cation exchange, 2 kbar 700°C

	$X_{\mathrm{Ca,pl}}$	$\mathrm{Ca}/(\mathrm{Ca}+\mathrm{Na})_{\mathrm{fl}}$
1	0.12–0.16	0.025
2	0.24–0.28	0.053
3	0.39–0.44	0.11
4	0.54–0.59	0.18
5	0.74–0.83	0.33
6	0.94–0.98	0.74
7	0.38	0.08–0.12

Where pl and fl refer to plagioclase and fluid.

2. Ternary feldspars, Elkins & Grove (1990)

	$X_{\mathrm{Ca,pl}}$	$X_{\mathrm{K,pl}}$	$X_{\mathrm{Ca,ksp}}$	$X_{\mathrm{K,ksp}}$	P kbar	T°C
8	0.33–0.50	0.018–0.09	0.01–0.04	0.75	2	800
9	0.31–0.46	0.022–0.09	0.01–0.04	0.73	2	800
10	0.30–0.43	0.025–0.13	0.01–0.04	0.71	2	800
11	0.38–0.46	0.025–0.10	0.01–0.049	0.67	1	800
12	0.24–0.33	0.06–0.12	0.02–0.057	0.56	1	890
13	0.72–0.76	0.0085–0.05	0.01–0.045	0.82	1	900
14	0.85–0.91	0.0027–0.05	0.01–0.041	0.89	1	890
15	0.10–0.16	0.10–0.20	0.01– 0.05	0.45	1	800

3. Alkali feldspar solvus: 2kb Orville, (1963), Luth & Tuttle (1966); 14 kb Goldsmith & Newton (1974)

	$X_{\mathrm{K,ab}}$	$X_{\mathrm{K,ksp}}$	P kbar	T°C
16	0.05–0.10	0.69–0.75	2	550
17	0.07–0.14	0.60–0.67	2	600
18	0.14–0.21	0.47–0.56	2	650
19	0.01–0.05	0.87–0.93	14	500
20	0.02–0.06	0.84–0.91	14	550
21	0.02–0.08	0.79–0.85	14	600

4. Plagioclase melting loop, Bowen (1913)

	$X_{\mathrm{Ca,L}}$	$X_{\mathrm{Ca,pl}}$	P kbar	T°C
22	0.04–0.07	0.27–0.34	0.001	1200
23	0.12–0.17	0.48–0.55	0.001	1300
24	0.31–0.34	0.68–0.73	0.001	1400
25	0.62–0.72	0.84–0.93	0.001	1500
26	0.0–0.02	0.0–0.05	0.001	1118
27	0.94–1.00	0.98–1.00	0.001	1551

5. Schliestedt & Johannes (1990) cation exchange

	$X_{\mathrm{Ca,pl}}$	$\mathrm{Ca}/(\mathrm{Ca}+\mathrm{Na})_{\mathrm{fl}}$	T°C	P kb
28	0.91–0.98	0.62	700	2
29	0.80–0.90	0.40	700	2
30	0.58–0.64	0.20	700	2
31	0.91–0.98	0.62	600	2
32	0.72–0.82	0.30	600	2
33	0.47–0.55	0.15	600	2
34	0.32–0.40	0.10	600	5
35	0.56–0.64	0.20	600	5
36	0.78–0.85	0.38	600	5

Where pl and fl refer to plagioclase and fluid.